

The Role of Hard Segment Content on the Molecular Dynamics of Poly(tetramethylene oxide)-Based Polyurethane Copolymers

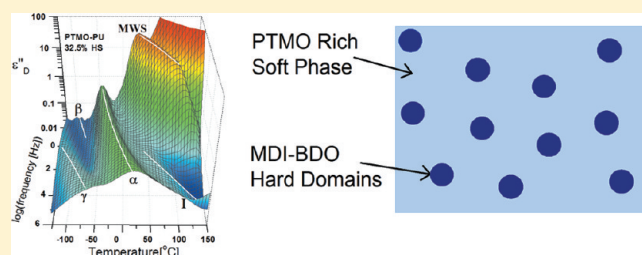
Alicia M. Castagna,[†] Daniel Fragiadakis,[‡] HyungKi Lee,[†] Taeyi Choi,[†] and James Runt^{*,†}

[†]Department of Materials Science and Engineering, The Pennsylvania State University, University Park, Pennsylvania 16802, United States

[‡]Naval Research Lab, Washington, D.C. 20375, United States

 Supporting Information

ABSTRACT: The effect of hard segment (4,4'-diphenylmethane diisocyanate–1,4-butanediol) content on the molecular dynamics of a series of PTMO-based segmented polyurethanes was investigated using broadband dielectric spectroscopy. The microphase-separated morphology and degrees of separation, extensively characterized in a previous publication, were utilized to aid in interpretation of the molecular dynamics. The soft phase segmental dynamics were observed to slow slightly, increase in breadth, and decrease in strength with increasing hard segment content: the influence of hard domains on the soft phase segmental dynamics is analogous to that of crystalline lamellae in semi-crystalline polymers. A Maxwell–Wagner–Sillars interfacial polarization process, arising from charge accumulation at hard/soft phase interfaces, was observed at higher temperatures. The strength of this process was found to be a rather sensitive indicator of the microphase mixing process.



INTRODUCTION

Segmented polyurethane (PU) copolymers are used extensively in applications ranging from foams and coatings to medical devices. These polymers can be synthesized from a wide variety of isocyanates, diol or diamine chain extenders, and macrodiols, using convenient addition polymerization methods. The nature of the polymerization generally yields “hard” segments with a rather broad distribution of sequence lengths. Consequently, polyurethane microphase separation and chain dynamics are quite complex as compared to diblock and triblock copolymers, in which the blocks have well-defined lengths and narrow polydispersity. Understanding the relationships between chemistry, morphology, and molecular dynamics is necessary in order to tailor material performance.

Depending on the block length, hard segment content, and chemical compatibility between the soft and hard segments, one can obtain polyurethane structures ranging from homogeneous to strongly phase separated.¹ Typically, the phase-separated structure consists of glassy (potentially crystalline) hard domains and an amorphous soft phase having a relatively low glass transition temperature (T_g).² The hard domains serve as physical cross-links in the soft matrix, leading to mechanical properties characteristic of elastomers for materials with relatively low hard segment contents.³ A significant number of studies have been carried out to understand the extent of microphase separation in PUs^{4–11} and its effect on properties. The molecular mobility of the polyurethane is strongly dependent on both the degree of phase separation, which determines the composition of hard and

soft domains, as well as the size and connectivity of the hard domains.^{12–15}

Poly(tetramethylene oxide) (PTMO) is a commonly used soft segment in polyurethanes due to its availability and well-characterized reactivity in polyurethane synthesis. The objective of the present study is to investigate the effect of hard segment content on the molecular dynamics of a series of well-defined PTMO-based segmented polyurethanes, where the concentration of 4,4'-diphenylmethane diisocyanate (MDI)–1,4-butanediol (BDO) hard segments is varied. Because of the complexity of these materials (multicomponent, multiphase systems with temperature and thermal history dependent microstructure), complete microstructural characterization is necessary in order to interpret the dynamics. To this end, the same PTMO soft segment PUs with the identical thermal history were used in the present study as were extensively characterized by Hernandez et al.¹¹ Their key microstructural characteristics are summarized in the initial portion of the Results and Discussion section. Although some research using dielectric spectroscopy on segmented polyurethanes has been reported,^{16–19} the present work is the first time that the dynamics have been investigated on PUs where all of the important details of the microstructure are known.

Received: July 25, 2011

Revised: August 18, 2011

EXPERIMENTAL SECTION

Materials. The series of segmented PUs were synthesized using an oligomeric poly(tetramethylene oxide) ($M_w = 1000$), 4,4'-diphenylmethane diisocyanate, and 1,4-butanediol using a two-step polymerization process by AorTech Biomaterials (Scoresby, QLD, Australia). PTMO–PU copolymers having four different hard segment contents (32.5, 40, 45, and 52 wt %) were investigated. Films were cast from a solution of the appropriate polymer in *N,N*-dimethylacetamide (DMAc, Biolab Australia, minimum 99% purity) and heated at 328 K for 16–18 h, followed by drying under vacuum at 313 K for another 24 h.

Thermal Analysis. Glass transition temperatures (T_g) were determined using a Seiko 220 differential scanning calorimeter. The response was measured over the temperature range of -90 to 100 °C at a heating rate of 10 °C/min under a nitrogen flow of 50 mL/min. The soft phase T_g was taken as the inflection point in the DSC thermogram from the first heating scan to be consistent with the thermal history of the DRS measurements.

Broadband Dielectric Relaxation Spectroscopy (DRS). Samples 0.1 – 0.2 mm thick were sandwiched between brass electrodes with a top electrode diameter of 2 cm in a parallel plate capacitor configuration. Isothermal relaxation spectra were collected under nitrogen using a Novocontrol GmbH Concept 40 BDRS spectrometer from 0.01 Hz to 10 MHz on heating from -120 to 200 °C.

Dielectric relaxation strength ($\Delta\epsilon$) and characteristic relaxation time (τ_{HN}) were determined for each relaxation process by fitting the dielectric loss to the appropriate form of the Havriliak–Negami (HN) function:

$$\epsilon''_{HN}(\omega) = \frac{\Delta\epsilon}{(1 + (i\tau_{HN}\omega)^a)^b} \quad (1)$$

where a and b are shape parameters where $0 < a, ab \leq 1$. The characteristic relaxation time is related to the maximum frequency of maximum loss by

$$f_{\max} = \left[\frac{1}{2\pi\tau_{HN}} \right] \left[\frac{\sin(\pi a/(2+2b))}{\sin(\pi ab/(2+2b))} \right]^{1/a} \quad (2)$$

Above T_g , the contribution from ohmic conduction arising from ionic impurities dominates the dielectric loss (ϵ''), potentially masking dipolar processes. This conduction contribution is not manifested in the real part of the dielectric response (ϵ'), and using a numerical approach, one can approximate the “conduction free” loss from ϵ' . We chose to apply the straightforward derivative method to achieve this, where the ohmic-conduction-free loss is determined from the logarithmic derivative of the dielectric constant:^{20,21}

$$\epsilon''_D = -\frac{\pi}{2} \frac{\partial \epsilon'(\omega)}{\partial \ln \omega} \quad (3)$$

Wubbenhorst et al. have shown that this method is a very good approximation of the “conduction-free” loss for relatively broad loss peaks like those observed here, while narrow peaks appear much narrower in ϵ''_D than in ϵ'' .²¹ The appropriate derivative form of the HN function was used to fit processes resolved by this method.²¹

RESULTS AND DISCUSSION

As noted earlier, the PTMO–PU copolymers under investigation are identical to those extensively characterized in an earlier publication, as is their thermal/process history.¹¹ In summary, discrete phase-separated hard domains (~ 10 nm in size) were observed for each PTMO–PU using tapping mode atomic force microscopy (AFM) (see Figure 1 for a representative AFM phase image). No hard segment crystallinity was detected in any of the copolymers using wide-angle X-ray diffraction.

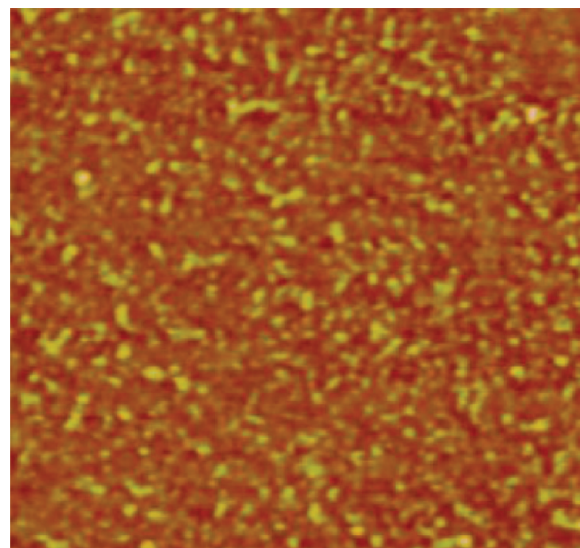


Figure 1. AFM phase image of PTMO–PU (HS 40%) from ref 11 at tapping force $r_{sp} = 0.85$. Scan size: 500×500 nm²; phase scale: 20° .

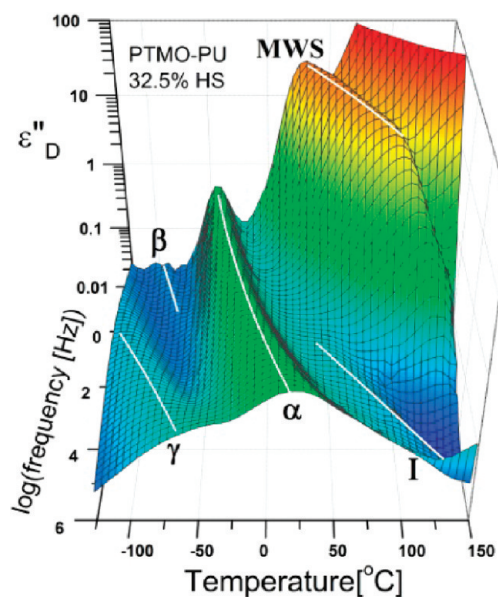


Figure 2. Frequency and temperature dependence of the conduction free dielectric loss for the PTMO copolymer containing 32.5% MDI–BDO hard segments.

Degrees of hard/soft segment demixing were quantified by using absolute scattering intensities from small-angle X-ray scattering (SAXS) experiments and the general model of Bonart and Müller.²² The degree of microphase separation in this approach is determined as the ratio of the experimental variance (scattering intensity) to the hypothetical completely phase separated value. Degrees of microphase separation for these and other similar PU copolymers are relatively low, and segregation of hard and soft segments is rather incomplete. In the work published in ref 11 the degrees of microphase separation were found to be ~ 0.30 for PTMO-32.5 and 40 and 0.35 for PTMO-45, consistent with the expectation of greater phase separation as mean hard segment length increases. However, kinetic constraints on segment demixing are known to be

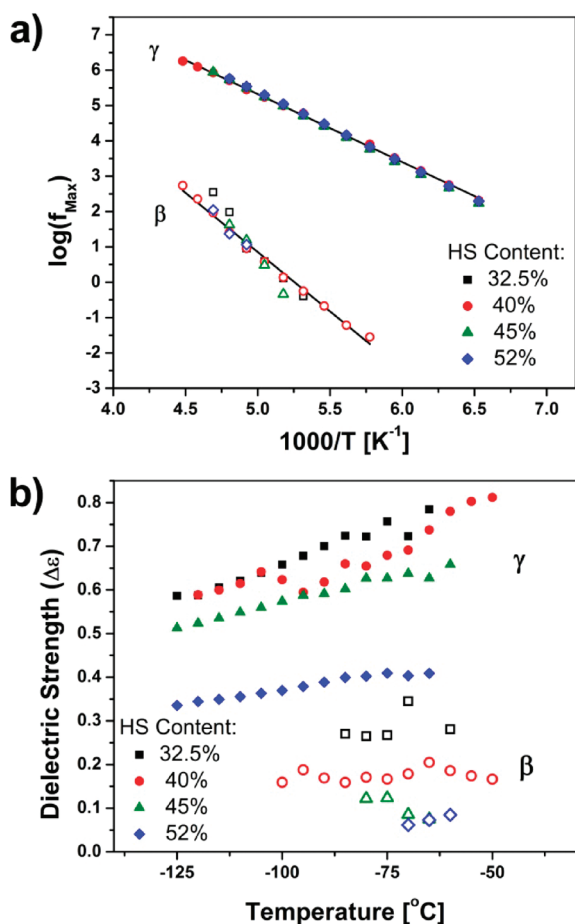


Figure 3. (a) Frequency maxima and (b) dielectric relaxation strengths of the γ (solid symbols) and β (open symbols) local relaxations.

important for PU copolymers having higher hard segment concentrations.^{23,24} Such an effect was observed for PTMO-52 in which the degree of microphase separation for PTMO-52 was determined to be rather small compared to the other PU–PTMO copolymers investigated in that study, 0.16. Since ~ 18 months had passed since the earlier study and the dielectric measurements reported herein, we were concerned that aging might result in an increase of phase separation during this time interval. SAXS experiments were consequently redone on the PTMO-45 and PTMO-52 copolymers. The degree of phase separation for PTMO-45 was identical within experimental uncertainty to that reported in ref 11. However, the measured SAXS invariant was found to be more than a factor of 2 larger for PTMO-52 at the time of the DRS experiments reported here and corresponds to a degree of phase separation of 0.36. As will be shown in the next section, this is entirely consistent with the measured dielectric relaxation behavior.

Broadband Dielectric Spectroscopy. Five relaxations are observed in dielectric loss spectra of all copolymers (see Figure 2 for an example): local glassy state motions (γ and β), segmental motion of the soft phase (α), an additional low-frequency relaxation (process I), and Maxwell–Wagner–Sillars interfacial polarization (MWS).

Glassy State Motions. The γ process is observed in the spectra of all PTMO–PU copolymers and arises from a local relaxation observed in the glassy soft phase associated with

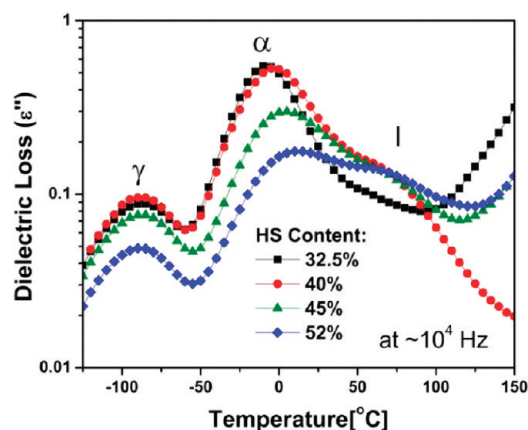


Figure 4. Dielectric loss as a function of temperature showing the γ , α , and I processes.

crankshaft motions of the ether oxygen containing segments.²⁵ It has an activation energy of 43 kJ/mol. The small, slower local process, β , with an activation energy of about 65 kJ/mol, is associated with reorientational motions of water molecules and is present in a wide variety of water-containing systems.^{26–29} For the case of hydrated polymers, the relaxation is also likely to involve local motions of the polymer chain segments where the water molecules are attached. Although the PUs were well dried prior to measurement, some residual water remains because of the strong interaction between the water molecules and the polar hard segments and ether linkages of the PTMO chain segments.

The relaxation times of the γ and β processes are not significantly affected by hard segment content (Figure 3a). The strength (Figure 3b) of the γ process decreases with increasing hard segment content, in keeping with the reduction in the PTMO content in the copolymers. The strength of the β process also decreases, indicating less residual water for the more highly phase-separated higher hard segment copolymers.

Soft Phase Segmental Motion and the “I” Process. At intermediate temperatures, two relaxation processes are observed: an α relaxation, associated with cooperative segmental motion of the soft segment-rich matrix, and the I process, which as will be described below is associated with the hard segments. The I process appears as a high-temperature/low-frequency shoulder off of the α process and is most clearly visible in the temperature domain (Figure 4), its strength relative to that of α relaxation increases with increasing hard segment content. Because of the overlap of the two processes, two HN functions are used to curve resolve these processes in the frequency domain.

As hard segment content increases, the strength of the soft phase α process decreases as expected (Figure 5c), and its breadth increases significantly (as does the interval associated with the change in heat capacity in DSC experiments, not shown): the HN parameter a decreases from ~ 0.45 to 0.2 with increasing hard segment content. This is most apparent when the process is normalized by the frequency and loss maxima (Figure 5a). This demonstrates that segments in the soft phase are relaxing in an increasingly heterogeneous manner. A reduction in strength, broadening, and slowing of the segmental relaxation is commonly observed for semicrystalline polymers as crystallinity increases; the influence of the hard domains on the

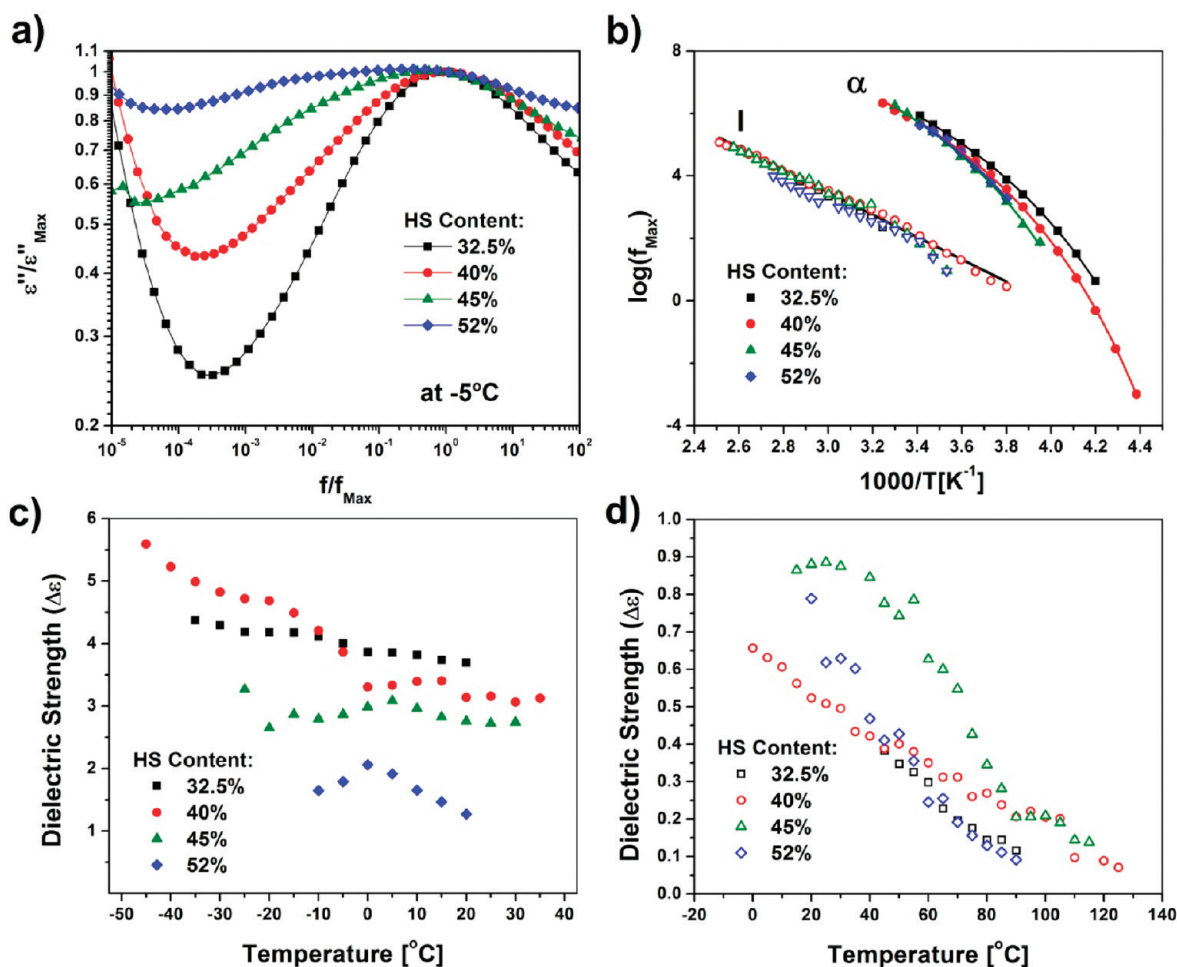


Figure 5. (a) Dielectric loss normalized by $\varepsilon''_{\text{Max}}$ and f_{Max} . (b) Arrhenius plot of the α (solid symbols) and I (open symbols) processes with VFT and Arrhenius fits, respectively. (c, d) Dielectric relaxation strengths of the α and I processes, respectively.

Table 1. Calorimetric T_g and Extrapolated T_g (T_{ref}) from DRS

	T_g (DSC) ± 3 °C	T_{ref} (at $\tau = 100$ s) ± 5 °C
HS 32.5%	−45	−48
HS 40%	−44	−44
HS 45%	−43	−38
HS 52%	−35	−39

segmental dynamics of these (amorphous) polyurethane copolymers is analogous to that of crystalline lamellae in semicrystalline systems.^{30,31}

The maxima of the α processes (Figure 5b) shift to somewhat lower frequencies with increasing hard segment content and follow a VFT temperature dependence:

$$f = f_0 \exp\left(\frac{B}{T - T_0}\right) \quad (4)$$

where T_0 is the Vogel temperature and f_0 is associated with vibration lifetimes³² and is fixed to 1.59×10^{11} Hz ($\tau_0 = 10^{-12}$ s) to reduce fitting uncertainties. The temperature coefficient B is related to the apparent activation energy ($E_a = BR/(1 - T_0/T)^2$)²⁰ and fragility. The T_g (T_{ref}) can be estimated from the segmental relaxation by extrapolating the VFT fit to $\tau = 100$ s

(see Table 1). T_{ref} increases rather modestly with increasing hard segment content, as does the T_g determined from DSC experiments, and T_g and T_{ref} are in good agreement for each copolymer within experimental error.

One would expect a hard domain α process (α_{hard}) to be observed in the DRS spectra, particularly in $\varepsilon''_{\text{der}}$ spectra in which losses arising from impurity ion conduction (which increases the loss significantly above the soft phase α process) are removed from the spectra. The I process is not associated with segmental motion in hard domains, however: it is observed at frequencies 3–4 decades lower than the segmental relaxation but follows an Arrhenius temperature dependence in the measured frequency range with an activation energy of about 70 kJ/mol. The frequency maximum of this relaxation is independent of hard segment content. Overlap of the I and soft phase α processes leads to some uncertainty in the fitted relaxation strengths, particularly the lower intensity I process. The fitted process I strengths for three of the copolymers are approximately the same, although those for PTMO-45 are somewhat greater than the others (Figure 5d). As will be described in the next section, a strong MWS relaxation is observed at temperatures above the I process, and it is likely that α_{hard} is obscured by the MWS relaxation.

A relaxation similar to process I has been observed for PTMO-based polyurethane networks and attributed to cold

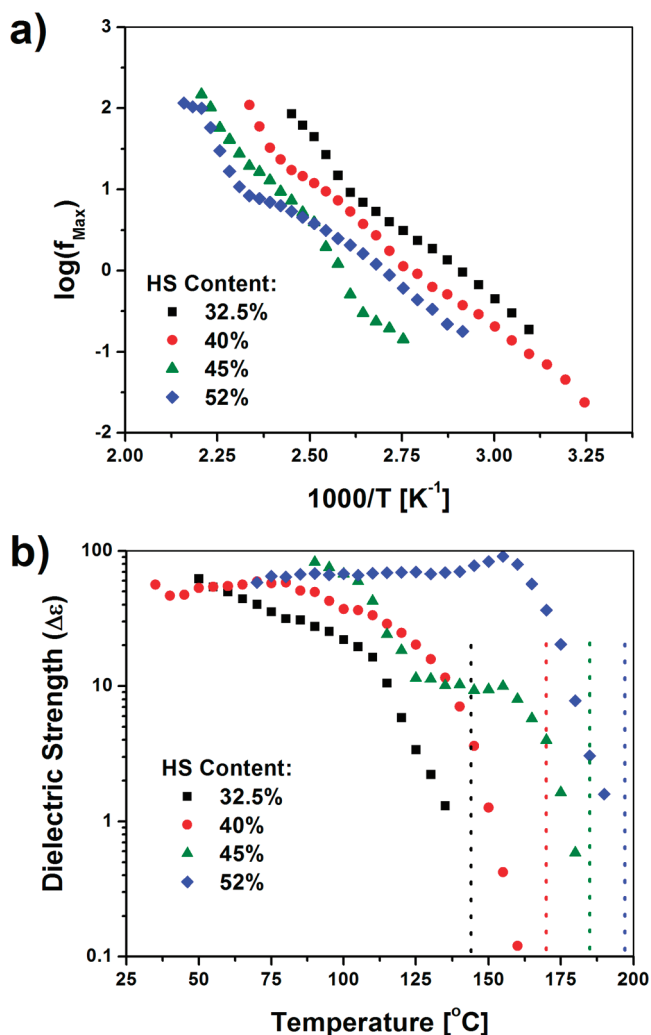


Figure 6. Temperature dependence of (a) the frequency maxima of the MWS process and (b) the dielectric relaxation strength with the end of the microphase mixing transition, indicated by dotted vertical lines.

crystallization of the PTMO soft segments,^{17,33} but this is not the origin in the present case since 1000 molecular weight PTMO soft segments are too short to crystallize in the PUs under investigation.¹¹ Another possibility is slow segmental motion of soft segments tethered at the boundaries of the hard phase, with restricted mobility. A similar process has been proposed in other microphase-separated PTMO-based polyurethanes³³ as well as in strongly aggregated Zn neutralized sulfonated polystyrene ionomers.³⁴ However, in some recent dielectric experiments, process I is observed at the same temperature/frequency position and with similar relaxation strength for MDI-BDO hard segment polyurethanes containing soft segments with widely varying chemistry³⁵ (e.g., polyether, poly(1,6-hexyl-1,2-ethyl carbonate), and predominately poly(dimethylsiloxane), making slow segmental motion of the soft phase an unlikely origin.

Given the Arrhenius temperature dependence and relatively large activation energy, we propose that process I is associated with local reorientations of the strongly H-bonded hard segment species within the hard domains. The decrease in strength of this process with increasing temperature can likely be attributed to the gradual release of constraints (hydrogen bonds between the hard segments).

Maxwell–Wagner–Sillars Interfacial Polarization. In heterogeneous materials with regions having different dielectric permittivity or conductivity, interfacial polarization occurs due to accumulation of charges at the interfaces.^{36–38} The accumulating charges behave similarly to a macroscopic dipole, giving rise to a dielectric loss peak (Maxwell–Wagner–Sillars (MWS) polarization). The MWS process appears in the frequency range of the loss dominated by dc conductivity of ionic impurities in soft phase. To resolve this process, the derivative formalism is applied, revealing a maximum in ϵ''_D . The frequency maxima and dielectric relaxation strength of the MWS process are shown in Figure 6 as a function of temperature. f_{max} and $\Delta\epsilon$ depend on the “contrast” between the soft matrix and hard domains, i.e., the difference between their respective dielectric constants and conductivities.

At low temperatures, $\Delta\epsilon_{\text{MWS}}$ exhibits large values (60–100), which are in the usual range for interfacial polarization of multiphase polymer systems.³⁹ On heating, $\Delta\epsilon_{\text{MWS}}$ gradually decreases (or, in the case of 52% hard segment, remains approximately constant) for several tens of degrees and then decreases rapidly. For some of the identical copolymers, we demonstrated previously (using temperature dependent synchrotron small-angle X-ray scattering) that these MDI-BDO-PTMO polyurethanes undergo phase mixing at elevated temperatures, signaled by a decrease in scattered intensity and finally the disappearance of the small-angle scattering peak.⁴⁰ This is a gradual process, taking place over a few tens of degrees. A complex and broad endotherm is also observed in DSC measurements in the same temperature range, associated with phase mixing.^{11,35} The temperature dependence of $\Delta\epsilon_{\text{MWS}}$ mirrors rather closely the behavior of the total scattered intensity in SAXS measurements. Therefore, it is possible to follow in detail the evolution of phase mixing using relatively simple dielectric measurements. The sharp drop-off in strength shifts to higher temperatures with increasing hard segment content and is very consistent with the end of the microphase mixing transition determined from the high-temperature DSC endotherm by Hernandez et al. (indicated by the dotted lines in Figure 5b).¹¹ This temperature shift is what is expected for higher hard segment copolymers: higher temperatures are required to solubilize the longer mean hard segment lengths in higher hard segment PTMO-PUs.

SUMMARY

Dielectric spectra of well-characterized MDI-BDO-PTMO polyurethane multiblock copolymers exhibit five dipolar relaxation processes. Of particular interest are the three that are observed at higher temperatures. The soft phase segmental relaxation is strongly affected by changing hard segment content, akin to the role of increasing crystallinity in semicrystalline polymers. Its strength is reduced and the relaxation broadens considerably with increasing hard segment fraction, demonstrating that the relaxing segments in the soft phase exist in an increasingly heterogeneous environment. The so-called process I, observed as a high-temperature shoulder off of the segmental process, likely originates from local reorientations of the strongly hydrogen-bonded segments in hard domains, in keeping with its Arrhenius temperature dependence and relatively large activation energy. A Maxwell–Wagner–Sillars interfacial polarization process is observed at the highest temperatures, its strength decreasing with increasing temperature, tracking quite well with

previous observations on hard/soft phase mixing from temperature dependent SAXS⁴⁰ and DSC.¹¹ The strength of the MWS process is demonstrated to provide a rather sensitive indicator of the microphase mixing process.

■ ASSOCIATED CONTENT

S Supporting Information. A discussion of the derivative method for calculating the conduction free dielectric loss for these materials. This material is available free of charge via the Internet at <http://pubs.acs.org>.

■ ACKNOWLEDGMENT

The authors gratefully acknowledge the support of the National Science Foundation, Polymers Program, under grant DMR-0907139. We also thank Dr. Ajay Padsalgikar and Ms. Jadwiga Weksler of AorTech Biomaterials for providing the copolymers used in our investigation.

■ REFERENCES

- (1) Eisenbach, C. D.; Gronski, W. *Makromol. Chem., Rapid Commun.* **1983**, *4* (11), 707–713.
- (2) Cooper, S. L.; Tobolsky, A. V. *J. Appl. Polym. Sci.* **1966**, *10* (12), 1837–1844.
- (3) Holden, G.; Legge, N. R.; Wuirk, R.; Schroeder, H. E. *Thermoplastic Elastomers*, 2nd ed.; Hanser Publisher: Munich, 1996.
- (4) Garrett, J. T.; Siedlecki, C. A.; Runt, J. *Macromolecules* **2001**, *34* (20), 7066–7070.
- (5) Hernandez, R.; Weksler, J.; Padsalgikar, A.; Runt, J. *Macromolecules* **2007**, *40* (15), 5441–5449.
- (6) Stevenson, J. C.; Cooper, S. L. *Macromolecules* **1988**, *21* (5), 1309–1316.
- (7) Vallance, M. A.; Castles, J. L.; Cooper, S. L. *Polymer* **1984**, *25* (12), 1734–1746.
- (8) Saiani, A.; Rochas, C.; Eeckhaut, G.; Daunch, W. A.; Leenslag, J. W.; Higgins, J. S. *Macromolecules* **2004**, *37* (4), 1411–1421.
- (9) Ezquerro, T. A.; Roslaniec, Z.; Lopez-Cabarcos, E.; Balta-Calleja, F. J. *Macromolecules* **1995**, *28* (13), 4516–4524.
- (10) Leung, L. M.; Koberstein, J. T. *J. Polym. Sci., Polym. Phys. Ed.* **1985**, *23* (9), 1883–1913.
- (11) Hernandez, R.; Weksler, J.; Padsalgikar, A.; Choi, T.; Angelo, E.; Lin, J. S.; Xu, L. C.; Siedlecki, C. A.; Runt, J. *Macromolecules* **2008**, *41* (24), 9767–9776.
- (12) Chang, A. L.; Briber, R. M.; Thomas, E. L.; Zdrachala, R. J.; Critchfield, F. E. *Polymer* **1982**, *23* (7), 1060–1068.
- (13) Garrett, J. T.; Xu, R.; Cho, J.; Runt, J. *Polymer* **2003**, *44* (9), 2711–2719.
- (14) Spathis, G.; Kontou, E.; Kefalas, V.; Apekis, L.; Christodoulides, C.; Pissis, P.; Ollivon, M.; Quinquenet, S. *J. Macromol. Sci., Part B: Phys.* **1990**, *29* (1), 31–48.
- (15) Ryan, A. J.; Stanford, J. L.; Still, R. H. *Polymer* **1991**, *32* (8), 1426–1439.
- (16) Pissis, P.; Georgoussis, G.; Bershtein, V. A.; Neagu, E.; Fainleib, A. M. *J. Non-Cryst. Solids* **2002**, *305*, 150–158.
- (17) Czech, P.; Okrasa, L.; Mechin, F.; Boiteux, G.; Ulanski, J. *Polymer* **2006**, *47* (20), 7207–7215.
- (18) Okrasa, L.; Czech, P.; Boiteux, G.; Mechin, F.; Ulanski, J. *Polymer* **2008**, *49* (11), 2662–2668.
- (19) Polizos, G.; Kyritsis, A.; Pissis, P.; Shilov, V. V.; Shevchenko, V. V. *Solid State Ionics* **2000**, *136*, 1139–1146.
- (20) van Turnhout, J.; Wubbenhorst, M. *J. Non-Cryst. Solids* **2002**, *305* (1–3), 50–58.
- (21) Wubbenhorst, M.; van Turnhout, J. *J. Non-Cryst. Solids* **2002**, *305* (1–3), 40–49.
- (22) Bonart, R.; Müller, E. H. *J. Macromol. Sci., Part B: Phys.* **1974**, *10* (1), 177–189.
- (23) Garrett, J. T.; Runt, J.; Lin, J. S. *Macromolecules* **2000**, *33* (17), 6353–6359.
- (24) Garrett, J. T.; Lin, J. S.; Runt, J. *Macromolecules* **2002**, *35* (1), 161–168.
- (25) Hedvig, P. *Dielectric Spectroscopy of Polymers*; Hilger: Bristol, 1977.
- (26) Cervený, S.; Alegría, A.; Colmenero, J. *Phys. Rev. E* **2008**, *77*, 031803.
- (27) Capaccioli, S.; Ngai, K. L.; Shinyashiki, N. *J. Phys. Chem. B* **2007**, *111* (28), 8197–8209.
- (28) Fragiadakis, D.; Runt, J. *Macromolecules* **2010**, *43* (2), 1028–1034.
- (29) Pissis, P.; Apekis, L.; Christodoulides, C.; Niaounakis, M.; Kyritsis, A.; Nedbal, J. *J. Polym. Sci., Part B: Polym. Phys.* **1996**, *34* (9), 1529–1539.
- (30) Ezquerro, T. A.; Baltà-Calleja, F. J.; Zachmann, H. G. *Polymer* **1994**, *35* (12), 2600–2606.
- (31) Ezquerro, T. A.; Liu, F.; Boyd, R. H.; Hsiao, B. S. *Polymer* **1997**, *38* (23), 5793–5800.
- (32) Santangelo, P. G.; Roland, C. M. *Macromolecules* **1998**, *31* (14), 4581–4585.
- (33) Raftopoulos, K. N.; Pandis, C.; Apekis, L.; Pissis, P.; Janowski, B.; Pielichowski, K.; Jaczewska, J. *Polymer* **2010**, *51* (3), 709–718.
- (34) Castagna, A. M.; Wang, W.; Winey, K. I.; Runt, J. *Macromolecules* **2011**, *44* (8), 2791–2798.
- (35) Fragiadakis, D.; Runt, J. To be published.
- (36) van Beek, L. K. H. *Dielectric Behavior of Heterogeneous Systems*; Heywood Books: London, 1967; Vol. 7.
- (37) North, A. M.; Pethrick, R. A.; Wilson, A. D. *Polymer* **1978**, *19*, 913–922.
- (38) Hayward, D.; Pethrick, R. A.; Siriwittayakorn, T. *Macromolecules* **1992**, *25* (5), 1480–1486.
- (39) North, A. M.; Pethrick, R. A.; Wilson, A. D. *Polymer* **1978**, *19*, 923–930.
- (40) Pongkitwitoon, S.; Hernández, R.; Weksler, J.; Padsalgikar, A.; Choi, T.; Runt, J. *Polymer* **2009**, *50* (26), 6305–6311.